Heliyon 10 (2024) e28811

Contents lists available at ScienceDirect

Heliyon

journal homepage: www.cell.com/heliyon

Research article

Evaluation of visible light and natural photosensitizers against *Staphylococcus epidermidis* and *Staphylococcus saprophyticus* planktonic cells and biofilm

Alisa Gricajeva [a,*], Irina Buchovec [b], Lilija Kalėdienė [a], Kazimieras Badokas [b], Pranciškus Vitta [b]

[a] *Institute of Biosciences, Department of Microbiology and Biotechnology, Life Sciences Center, Vilnius University, Sauletekio avenue 7, LT-10257, Vilnius, Lithuania*

[b] *Institute of Photonics and Nanotechnology, Faculty of Physics, Sauletekio avenue 3, LT-10257, Vilnius University, Vilnius, Lithuania*

ARTICLE INFO

Keywords:
staphylococci
bacterial biofilms
antimicrobial photoinactivation
riboflavin
chlorophyllin
superoxide anion detection

ABSTRACT

Antimicrobial photoinactivation (API) has shown some promise in potentially treating different nosocomial bacterial infections, however, its application on staphylococci, especially other than *Staphylococcus aureus* or methicillin-resistant *S. aureus* (MRSA) species is still limited. Although *S. aureus* is a well-known and important nosocomial pathogen, several other species of the genus, particularly coagulase-negative *Staphylococcus* (CNS) species such as *Staphylococcus epidermidis* and *Staphylococcus saprophyticus*, can also cause healthcare-associated infections and foodborne intoxications. CNS are often involved in resilient biofilm formation on medical devices and can cause infections in patients with compromised immune systems or those undergoing invasive procedures. In this study, the effects of chlorophyllin and riboflavin-mediated API on *S. epidermidis* and *S. saprophyticus* planktonic cells and biofilm are demonstrated for the first time. Based on the residual growth determination and metabolic reduction ability changes, higher inactivating efficiency of chlorophyllin-mediated API was determined against the planktonic cells of both tested species of bacteria and against *S. saprophyticus* biofilm. Some insights on whether aqueous solutions of riboflavin and chlorophyllin, when illuminated with optimal exciting wavelength (440 nm and 402 nm, respectively) generate $O_2^{-\bullet}$, are also provided in this work.

1. Introduction

Hospital-acquired infections (HAI) are considered a major issue globally, with various types of bacteria exerting the highest impact on the occurrence of these infections. Different *Staphylococcus* spp., which form a part of human natural skin microbiota, have been very often isolated from diverse clinical sources and form a clinically significant group of bacteria causing nosocomial infections [[1–4]]. Among all the staphylococci (staph) group, *Staphylococcus aureus* is the most renowned pathogen, contributing to dangerous human and animal infections, including bloodstream infections and foodborne intoxications (FI). MRSA is the most significant concern in HAI [[5,6]], nevertheless, several other staph species can also cause nosocomial infections, as well as FI, although they may not be as common or well-known and investigated as *S. aureus* [[7,8]]. Some of these species include CNS, such as *Staphylococcus epidermidis*

* Corresponding author.
E-mail address: alisa.gricajeva@gmc.vu.lt (A. Gricajeva).

https://doi.org/10.1016/j.heliyon.2024.e28811
Received 8 November 2023; Received in revised form 21 March 2024; Accepted 25 March 2024
Available online 30 March 2024

and *Staphylococcus saprophyticus* [[9,10]]. *S. epidermidis* - one of the most abundant commensal bacteria of human skin and mucosae, is also a common cause of healthcare-associated severe infections in immunocompromised patients, especially associated with the use of indwelling medical devices (central venous catheters, urinary catheters, prosthetic joints), that frequently serve as a scaffold for the formation of biofilms [[11,12]]. While *S. saprophyticus* is primarily known as a cause of urinary tract infections (UTIs) in women, it can also be implicated in healthcare associated UTIs and FI. Furthermore, *S. saprophyticus* is also capable of forming biofilms, which can contribute to the persistence and recurrence of infections, especially in the context of medical devices. Managing and treating biofilm-associated infections is a complex challenge due to their antibiotic-resistance and the protective nature of the biofilm matrix [[13–15]]. Therefore, ongoing research and advancements in infection control and treatment strategies are critical in addressing these infections effectively and safely [[14,16]].

Antimicrobial photodynamic inactivation (API) shows promise as a treatment of localized infections caused by different types of bacteria and fungi [17]. API involves using a harmless (non-toxic), light-absorbing compound known as photosensitizer (PS), molecular oxygen, and visible light. This approach seems to have great potential for reducing the need for antibiotics and minimizing the risk of antibiotic resistance. Usually, when the PS absorbs light, it enters a triplet state and then interacts with molecular oxygen. This interaction can produce reactive oxygen species (ROS), causing oxidative stress and cellular damage that destroys bacterial cells. Several different ROS types can form, such as singlet oxygen ($^1O_2$) belonging to the type II pathway, superoxide anion ($O_2^{-\bullet}$), hydrogen peroxide (H_2O_2), and hydroxyl radical ($^\bullet OH$) characteristic to the type I pathway [18]. Each ROS type plays a different role in the API process and can have other effects on bacterial cells. The $O_2^{-\bullet}$ is a primary oxygen radical generated in bacterial cells when O_2 molecule acquires an electron. Following this, the $O_2^{-\bullet}$ can activate formation of a ROS cascade such as free $^\bullet OH$, the most dangerous ROS interacting with virtually any organic substance in the cell [[19–22]].

Because of its multitarget action, one of the significant benefits of API is low likelihood of bacteria to develop resistance, rendering it safe for use in various settings such as hospitals, food environments, etc. [[23–27]]. For the inactivation of both free-floating (planktonic) and sessile forms (biofilms) of bacteria that can be human-associated, natural, non-toxic, and easy-to-produce PSs are preferred. Currently, curcumin, riboflavin (RF), perylenequinones, psoralens [28], and, most recently, studies have shown that chlorophyll derivatives like chlorophyllins (Chl), are effective natural PSs that can be used for API [[29–32]]. One of the safest and most harmless to human natural PSs are RF and Chl [29]. Both RF (natural water-soluble compound, vitamin B2) and Chl (water--soluble, can be extracted from plants, E 140 (ii)) are light-sensitive (photoactive) compounds mainly used as food dyes [[33,34]]. Nevertheless, studies and applications of the RF- and Chl-mediated APIs (RF-API and Chl-API, respectively) to control *S. epidermidis* and *S. saprophyticus*, their planktonic cells, and biofilms remain scarce. There are some previous studies that have shown RF- (using UV-A and blue light irradiation) and Chl-API have antibacterial effects on *S. aureus* and MRSA planktonic cells and biofilms [[35,36]]. The high efficiency of RF-API was also shown by Thakuri et al. (2011), who used circularly organized 65-blue LED array designed as the light source [37]. Most recently, photo-illuminated (at 450 nm - blue light) RF was shown to have biofilm-disrupting activity against both mono and mix *S. aureus* and *E. coli* biofilms [38]. Chl-mediated API was reported to be effective against *S. aureus* for food preservation and decontamination [[39,40]]. Several other studies have also indicated an effective inactivation of planktonic *S. aureus* cells by photosensitized chlorophyllin copper sodium salt [41], or chlorophyllin sodium magnesium salt, which has a superior antimicrobial activity to the former under irradiation of blue light [42]. Hasenleitner and Plaetzer (2019) and Caires et al. (2020) demonstrated the inactivation of planktonic *S. aureus* and MRSA cells, respectively, by a combination of red-light with chlorophyllin sodium magnesium salt [[43,44]]. However, some most popular PSs for API of *S. aureus* as well as *S. epidermidis* and *S. saprophyticus* planktonic cells and biofilms are reported to be methylene blue, toluidine blue, rose bengal, porphyrins and some natural pigments [[45–56]]. Therefore, the aim of this study was to investigate the effect of RF- and Chl-mediated APIs on *S. epidermidis* (planktonic cells) and *S. saprophyticus* (planktonic cells and biofilms). Residual viability determination involving CFU count and alamarBlue™ reduction methods showed that Chl-mediated API was more efficient on all tested model bacterial strains and tested cell forms (planktonic cells and biofilms). Furthermore, although it is known that during the photoactivation of Chl various types of ROS (predominantly $^1O_2$) are formed, no research has been performed on the ability of Chl to generate $O_2^{-\bullet}$ after irradiation. Since the role of $O_2^{-\bullet}$ is no less important, some insights into whether it forms during the light activation (photoactivation) of RF and Chl by 440 nm and 402 nm (visible light), respectively, are also provided in this work.

2. Methods

2.1. Photosensitizers (PS)

Non-copperized chlorophyllin magnesium sodium salt (Chl) and RF were purchased from Carl Roth (Germany) and Sigma-Aldrich (USA), respectively. For Chl- and RF-APIs, 0.15 mM Chl (pH 6.8) and 0.11 mM RF (pH 6.2) aqueous stock solution were used [24]. All working PS solutions were freshly prepared by diluting them with 0.01 M PBS buffer (pH 7.4) (Carl Roth, Germany) just before the experiments. Since PSs are photosensitive compounds, dark conditions were maintained during their handling before photoinactivation experiments.

2.2. Light source

For the API experiments a LED-based light source with the emission maxima at 440 nm and 402 nm corresponding to the RF and Chl absorption maxima, respectively, was used [32]. The light irradiance at the samples' surfaces (at a 7 cm distance) was 5 (for planktonic cells), 20, and 25 mW/cm^2 (used for biofilms with RF and Chl). Irradiation doses (J/cm^2) were calculated as the product of the

intensity (mW/cm^2) and the irradiation time (seconds). The calculations of the irradiation doses for the experiments are shown in Table 1.

2.3. Detection of superoxide anion ($O_2^{-\bullet}$) in solution

The nitroblue tetrazolium (NBT) reduction assay is a commonly used method to detect and quantify the production of superoxide anion ($O_2^{-\bullet}$) in biological samples [[21,22]]. NBT reduction was accomplished according to Cheng's and Liang's method [[57,58]], with minor modifications. According to this method, NBT reduction occurs during its irradiation in a solution with a PS. During the reduction, generated $O_2^{-\bullet}$ and NBT form a blue formazan in the solution, the absorption of which is observed at 560 nm.

All solutions were prepared in 50 mM PBS (pH 7.4) buffer. 3 mL of the reactant contained 0.011 mM RF or Chl, 10 mM L-methionine (electron donor) (Carl Roth, Germany), and 0.16 mM NBT 161 (Carl Roth, Germany). According to Cheng's and Liang's methodology [[57–59]], 0.0024 mM concentration of PSs was also analyzed. The prepared solutions were illuminated with a source of visible light (Section 2.2.) by adjusting the wavelength optimally exciting PSs (RF - 440 nm, Chl - 402 nm). In the controls, the reactant was stored in the dark.

Also, the inhibition of NBT reduction was performed after using $O_2^{-\bullet}$ binding agent gallic acid (Carl Roth, Germany) [57]. 100 mM of gallic acid was added to the 20 ml NBT reduction solutions prepared. The combined solutions underwent irradiation with visible light at the suitable wavelength, at an intensity of 5 mW/cm^2 and the absorption spectra of all samples were measured using a UV-VIS-NIR spectrophotometer (LAMBDA 950, PerkinElmer, USA). Measurements were conducted in polymethyl methacrylate cuvettes with a path length of 1 cm.

2.4. Microorganisms used in this work

For the evaluation of Chl- and RF-mediated API Gram-positive bacteria were chosen as model microorganisms for the study. Names of the species and some of their important properties are presented in Table 2.

2.5. Cultivation conditions and preparation of planktonic cells and biofilms for API

For the achievement of the planktonic cell suspensions of *S. epidermidis* ATCC 12228 and *S. saprophyticus* AG1, bacteria were cultivated in Luria Bertani (LB) (Carl Roth, Germany) liquid media at 37 °C with 180–200 rpm agitation in thermal shaker (IKA, Germany) overnight. The overnight inoculums of the bacteria were then added to a fresh LB media and cultivated in identical conditions as mentioned until the optical density at 600 nm (OD_{600}) corresponding to 10^{8-9} CFU/mL was achieved. Then bacterial pellet was collected via centrifugation (3 min at 9000×*g*), resuspended in 0.01 M PBS (pH 7.4) and used for the API experiments instantly (Section 2.5.1).

For the formation of monocultural *S. saprophyticus* AG1 biofilms, 10^8 CFU/mL bacterial suspensions were used: 100 μL of the bacterial suspension was dispensed into flat-bottom radiation-sterilized 96-well polystyrene microtiter plate (MtP) wells. Further, for the formation of the biofilms MtP were incubated in static conditions at 37 °C for 22 h. To remove the planktonic cells which can affect the results, formed *S. saprophyticus* AG1 biofilms were washed three times with 0.01 M PBS (pH 7.4). Further, washed biofilms were utilized for the RF- and API experiments (Section 2.5.2). The formation of *S. saprophyticus* AG1 biofilms was confirmed following staining with a 0.1% crystal violet solution [[62,63]].

Table 1
Irradiation doses used in this work.

Time (min)	Irradiation dose (J/cm^2)		
	402 nm/440 nm Irradiance 5 mW/cm^2	402 nm Irradiance 20 mW/cm^2	440 nm Irradiance 25 mW/cm^2
1	0.3	n/u	n/u
2	0.6	n/u	n/u
5	1.5	n/u	n/u
10	3	n/u	n/u
20	6	n/u	n/u
30	9	36	45
45	13.5	n/u	n/u
60	18	72	90
75	22.5	n/u	n/u
90	n/u	108	135
120	36	144	180
150	45	n/u	n/u
200	60	n/u	n/u
240	72	n/u	n/u
300	90	n/u	n/u

*n/u – not used.

Table 2
Microorganisms used in this work.

Species name	Source and short description	Biofilm formation ability
Staphylococcus epidermidis ATCC 12228	American Type Culture Collection (ATCC) reference strain deposited by FDA. The culture has applications in bioinformatics, food testing, media testing, and quality control, and it is a microbiome standard component [*Staphylococcus epidermidis* (Winslow and Winslow) Evans (ATCC 12228)]	no [60]
Staphylococcus saprophyticus AG1	Strain previously isolated, characterized [61] and deposited at a Department of Microbiology and Biotechnology (Vilnius University) microorganism collection (Genome accession nr. at NCBI: PRJNA513961). Species is known to cause uncomplicated urinary tract infections (UTI) with biofilm-formation ability being critical for these pathogens to cause UTI [14].	yes

2.5.1. Photoinactivation of planktonic cells

For the RF- and Chl-mediated photoinactivation of the planktonic cells of *S. epidermidis* ATCC 12228 and *S. saprophyticus* AG1, their cells were resuspended in 0.011 mM RF (pH 7.4) or 0.015 mM Chl (pH 7.4) to a 10^7 CFU/mL concentration. As a control, bacteria resuspended in 0.01 M PBS (pH 7.4) were used. All prepared mixtures in quantities of 200 μL were pipetted into MtP (as described in 2.5) and irradiated reaching doses described in Table 1. At each irradiation step sampled bacterial suspensions were diluted, spread on LB agar plates, and incubated at 37 °C for 16–36 h. The numbers of surviving (residual) bacteria (CFU/mL) were transformed to $\log_{10}$ scale. CFU/mL counts of the bacterial cells that were kept in the dark (dark controls) with or without RF, Chl or PBS were also determined.

2.5.2. Photoinactivation of biofilms

The MtPs with pre-formed (as it was described in Section 2.5) *S. saprophyticus* AG1 biofilms were filled with 200 μL of 0.011 mM RF (pH 7.4), 0.015 mM Chl (pH 7.4) or 0.01 M PBS (pH 7.4). After that biofilms were immediately irradiated with $\lambda = 440$ nm at 25 mW/cm^2 or $\lambda = 402$ nm at 20 mW/cm^2 for the RF- and Chl-based API, respectively. Biofilms were subjected to various levels of illumination exposure (refer to Table 1). During each sampling step, bacterial biofilms were detached from the walls of the MtP, vigorously vortexed, and then diluted. Subsequently, the viability of the bacteria was determined by counting CFU on LB agar plates in conditions described in Section 2.5.1. The surviving bacterial counts (CFU/mL) were converted to a $\log_{10}$ scale. Additionally, CFU counts of biofilm-forming cells that were kept in the dark with or without RF, Chl or PBS were also determined.

2.6. Viability assay of photoinactivated bacteria using alamarBlue™

Viability of the investigated staphylococcal planktonic cells and biofilms after APIs was also evaluated by their ability to reduce alamarBlue™ (resazurin-based compound) (Invitrogen, USA). Planktonic *S. epidermidis* ATCC 12228 and *S. saprophyticus* AG1 cells and *S. saprophyticus* AG1 biofilm were photoinactivated as described in Sections 2.5.1 and 2.5.2. Biofilms, before adding to alamarBlue™, were mechanically detached using sterile micropipette tip from the walls of MtP's and vigorously vortexed. The proportions of the volume of alamarBlue™ and bacteria (planktonic cells or mechanically detached biofilms), sampled at the appropriate time points was 1:10. Combined dye and bacteria samples were incubated 3 h at 37 °C and the alterations in their fluorescence were quantified by a TFS Verioscan Flash (USA) plate reader. Fluorescence was assessed by exciting the samples at 560 nm and detecting emission at 590 nm. The measurements were carried out in flat-bottomed 96-well polystyrene MtPs (Fisher Brand, USA). The percentage reduction of alamarBlue™ by fluorescence, which indicates cell viability across all tested groups which underwent RF-mediated and Chl-mediated API was determined as described previously [24].

2.7. Scanning electron microscopy (SEM) of S. saprophyticus AG1 biofilm

The influence of used APIs on the morphology of *S. saprophyticus* AG1 biofilms grown in MtP (as described in Section 2.5) was investigated by SEM (CamScan Apollo 300, Cambridge, UK). Biofilms with a 3 $\log_{10}$ decrease in cell viability after exposure to 25 mW/cm^2 for 93 min (RF-API) and 20 mW/cm^2 for 60 min (Chl-API) were selected for SEM. The irradiated biofilms and untreated control biofilms were carefully mechanically separated from the walls of the MtPs, and 10 μl of each sample was dropped onto the tip of the SEM stub covered with copper foil tape. The samples were then dried at ambient temperature and coated with gold (50 nm) using a Q150T ES sputter coater (Quorum Technologies, Lewes, England). The scanning was carried out using an electron beam with 20 kV accelerating voltage.

2.8. Statistical analysis

All experiments included at least three independent biological and technical replicates and were given providing mean ± SD. Students t-test and one-way ANOVA were applied as statistical tests. Statistically significant differences between tested groups were considered when $p \leq 0.05$. Graphs were constructed using Origin Pro 8.1 (OriginLab Corporation, USA) and GraphPad Prism V. 6 (GraphPad Software, USA) software. Statistical analysis was carried out using GraphPad Prism V. 7.

3. Results and discussion

3.1. Detection of superoxide anion

Various ROS generated during API may have different phototoxic effects on the same strain of bacteria, depending on the type of PS used and the medium conditions [19]. When the PS is exposed to specific wavelengths of light, it becomes excited and transfers its energy to molecular oxygen, generating ROS. Superoxide anions ($O_2^{\bullet-}$) are among the ROS produced in this process. $O_2^{\bullet-}$ is a highly reactive and short-lived free radical important in various biochemical and physiological processes. It can cause damage to different cellular components, including lipid membranes, proteins, and DNA. Detecting $O_2^{\bullet-}$ in solution typically requires specialized methods and reagents due to its reactivity. We determined the formation of $O_2^{\bullet-}$ by optical spectroscopy by analyzing the degree of reduction of NBT, which readily reacts with $O_2^{\bullet-}$ [21]. It is generally known that RF can generate $O_2^{\bullet-}$ when exposed to visible or UV light in the presence of O_2 [[57,64]]. This phenomenon occurs due to the photoexcitation of RF molecules, forming excited states that can react with oxygen to produce superoxide radicals. However, there is no research regarding the ability of non-copperized magnesium sodium chlorophyllin (Chl) to generate $O_2^{\bullet-}$ after irradiation. Fig. 1 displays the impact of irradiating visible light at wavelengths of 440 nm and 402 nm on the reduction of NBT during the photochemical reaction of RF and Chl, respectively. First, we determined and compared the formation of $O_2^{\bullet-}$ after irradiation of 0.0024 mM RF and Chl (Fig. 1, A).

As shown in Fig. 1 (A), the amount of reduced NBT at 560 nm increased after exposure to RF with 440 nm light (5 mW/cm^2 irradiance). This means that the amount of $O_2^{\bullet-}$ produced increases accordingly. After 0.6 J/cm^2 light exposure (irradiation for 2 min), the absorbance at 560 nm increased to 0.55, which means that type I ROS $O_2^{\bullet-}$ was formed. Cheng et al. (2015), applying the same irradiation dose of 0.6 J/cm^2 (1 mW/cm^2 irradiance), obtained 0.7 value absorption at 560 nm [57]. This absorption value differs from our work by 1.3 times. This can be explained by the fact that the irradiation dose was the same, but the irradiation time was longer and reached 10 min. When the irradiation dose was increased to 9 J/cm^2, the optical density at 560 nm reached 1.75, indicating the increase of the amount of $O_2^{\bullet-}$.

Compared with the RF, following exposure to irradiation of 0.0024 mM Chl with 402 nm light, up to 7 times lower level of NBT reduction was obtained. After exposure to 9 J/cm^2 irradiation (5 mW/cm^2 irradiance), the absorbance value at 560 nm increased only to 0.25, indicating reduction of NBT and formation of $O_2^{\bullet-}$ (Fig. 1, A). There is data in the literature that both types of photochemical reactions occur during Chl-API, but type II reactions, during which $^1O_2$ is formed, predominate [[29,30,65]]. Although a small generation of $O_2^{\bullet-}$ was obtained in the work, it shows that during the photoactivation of Chl by 402 nm light, the Chl radical transfers the newly acquired electron to oxygen as a result superoxide radicals are forming.

Also, the 0.011 mM concentration of both PSs was analyzed. The irradiation of 0.011 mM RF with blue light at 440 nm produced a high amount of $O_2^{\bullet-}$, while in the case of 0.011 mM Chl, the amount of $O_2^{\bullet-}$ did not reach the same level even after a 6-fold increase in the irradiation dose with near UV 402 nm at light (Fig. 1, B).

When a $O_2^{\bullet-}$ binding agent, such as gallic acid, is added to the solution, a decrease in NBT reduction can be detected, indicating the inhibition of this reduction process [58]. Gallic acid is a polyphenol compound that can act as an antioxidant by donating electrons to neutralize free radicals. It can scavenge $O_2^{\bullet-}$ by reducing them to less harmful substances. Fig. 1 show the scavenging activity of $O_2^{\bullet-}$ using 100 mM concentration of gallic acid. When gallic acid was introduced into the NBT/PS (RF or Chl) solutions, no absorption at 560 nm occurred after all light exposures were applied. This means that after using gallic acid, the reduction of NBT was inhibited; that is, the binding of superoxide anions formed after irradiation occurred.

In summary, obtained results suggest that irradiating RF with 440 nm blue light produces more $O_2^{\bullet-}$ than irradiating Chl with 402

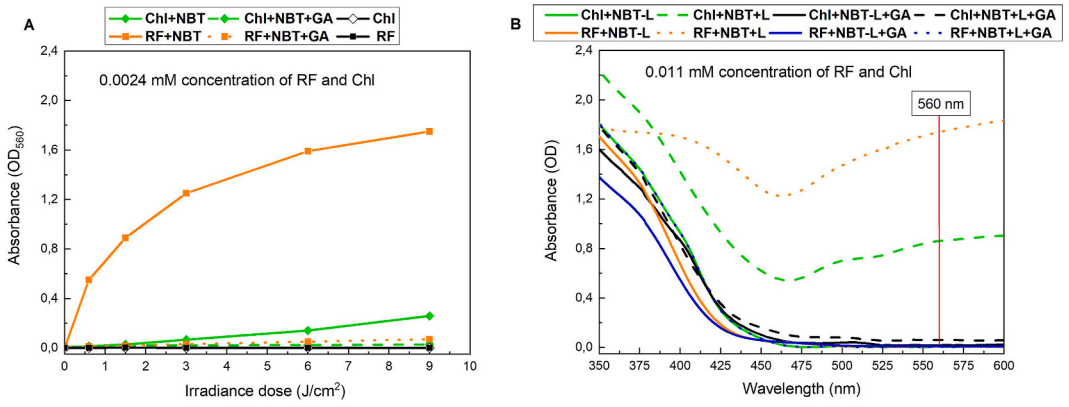

Fig. 1. Effects of visible light irradiation at 5 mW/cm^2 on NBT reduction by PSs photochemical treatment and $O_2^{\bullet-}$ scavenging activity of 100 mM gallic acid: (**A**) dependence on irradiation dose (440 nm blue light for 0.0024 mM RF and 402 nm near UV light for 0.0024 mM Chl); (**B**) spectra of PSs upon irradiation of 0.011 mM RF by 9 J/cm^2 irradiation dose at 440 nm blue light and of 0.011 mM Chl by 36 J/cm^2 irradiation dose at near UV light. RF-riboflavin; Chl-chlorophyllin; NBT-nitro blue tetrazolium; GA-gallic acid; L-light. (For interpretation of the references to color in this figure legend, the reader is referred to the Web version of this article.)

nm near-UV light. This suggests that during Chl-API at lower irradiation doses, the formation of $^1O_2$ is likely to dominate initially. However, after applying higher irradiation doses, when Chl has already been photodegraded [[24,31]], and the amount of molecular oxygen in the solutions has decreased, more $O_2^{\bullet-}$ began to form. All this can influence the antibacterial effect of the API.

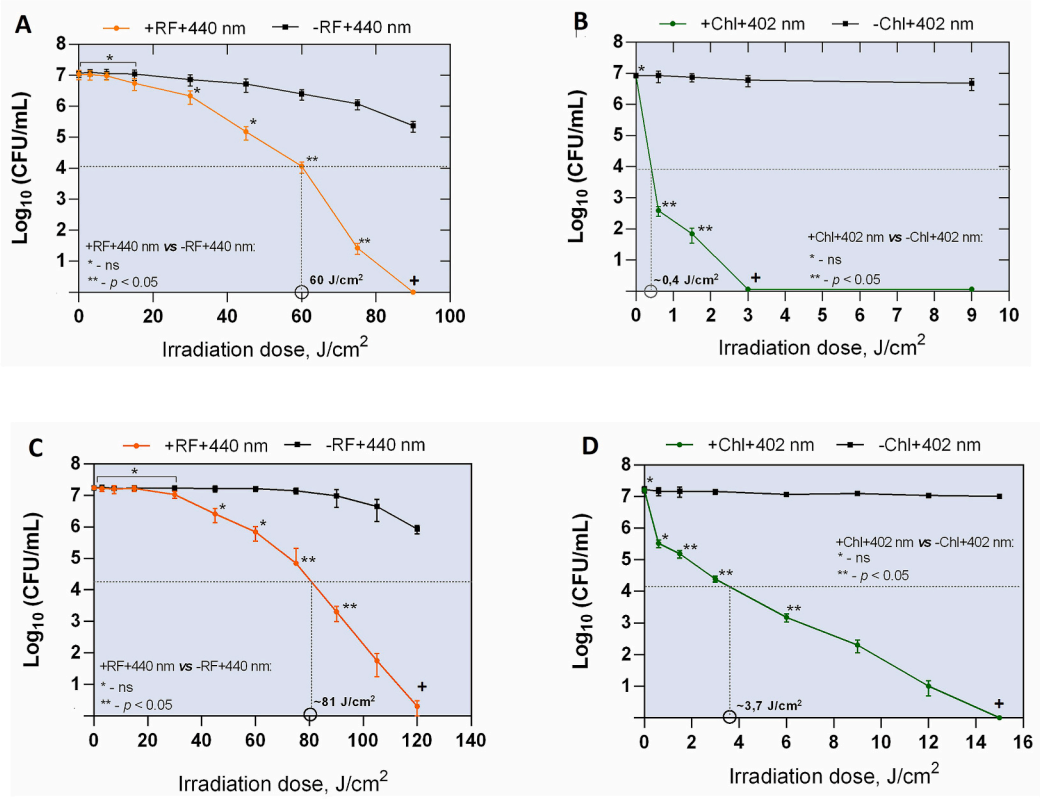

E

Strain \ Incubation time, min	Planktonic cells: +RF-440 nm* Log_{10} (CFU/mL) 2	5	10	30	60	80	-RF-440 nm** Log_{10} (CFU/mL) 2	5	10	30	60	80
S. epidermidis ATCC 12228	7.1±0.7	7.1±0.4	7.0±0.6	7.1±0.6	7.1±0.4	n	7.1±0.6	7.2±0.6	7.1±0.8	7.1±0.5	7.1±0.2	n
S. saprophyticus AG1	7.3±1.2	7.2±0.9	7.2±0.7	7.2±0.7	7.2±0.9	7.2±1.2	7.3±1.2	7.3±1.1	7.2±0.7	7.2±0.7	7.2±0.9	7.2±1.2
Strain \ Incubation time, min	+Chl-402 nm* Log_{10} (CFU/mL) 2	5	10	30	60	80	-Chl-402 nm** Log_{10} (CFU/mL) 2	5	10	30	60	80
S. epidermidis ATCC 12228	6.9±0.7	6.9±0.8	6.9±0.5	n	n	n	6.9±0.9	6.9±0.7	6.9±0.9	n	n	n
S. saprophyticus AG1	7.3±1.0	7.2±1.0	7.3±0.7	7.3±0.9	7.3±1.2	7.3±1.3	7.2±1.0	7.3±0.8	7.2±0.9	7.2±1.1	7.3±0.8	7.2±1.4

Fig. 2. **(A)** RF-API and (**B**) Chl-API of the planktonic cells of *S. epidermidis* ATCC 12228; (**C**) RF-API and (**D**) Chl-API of the planktonic cells of *S. saprophyticus* AG1. A horizontal dashed line in the graphs denotes minimal 3 log_{10} reduction (indicating bactericidal effect). Black circles on the x axis indicate the minimal illumination doses required for the bactericidal effect. ns – non-significant; + - the points are below the detection limit. (**E**) CFU counts of dark controls (reported in log_{10} scale) of the planktonic cells of *S. epidermidis* ATCC 12228 and *S. saprophyticus* AG1.* - dark control with RF or Chl, respectively; ** - dark control without RF or Chl, respectively; n – was not evaluated; +RF+440 nm *vs* + RF-440 nm and –RF-440 nm or + Chl+402 nm *vs* + Chl-402 nm and –Chl-402 nm p value < 0.05.

3.2. Results of bacteria photoinactivation

3.2.1. Inactivation of planktonic cells

For the investigation of the impact of the RF- and Chl-API on *S. epidermidis* ATCC 12228 and *S. saprophyticus* AG1 planktonic cells, irradiation doses were varied from 0.3 J/m^2 to 180 J/m^2 at 440 nm (for the RF-mediated API) and 402 nm (for the Chl-mediated API), respectively, depending on the response of the bacteria.

The reduction of ≥3 $\log_{10}$ (by 99,9%) of bacteria is recognized as a bactericidal effect [NCCLS, M26-A Standard] [[66,67]]. Therefore, the minimal doses of exposure to irradiation at 440 nm causing ≥3 $\log_{10}$ reduction using RF-API against the planktonic cells of the selected model bacteria were determined to be 60 J/cm^2 for the *S. epidermidis* ATCC 12228 and ~81 J/cm^2 for *S. saprophyticus* AG1 (Fig. 2, A and C, respectively). Chl-API bactericidal effect on *S. saprophyticus* AG1 required an irradiation dose of ~3.7 J/cm^2 at 402 nm and less than 0.4 J/cm^2 for the *S. epidermidis* ATCC 12228 planktonic cells (Fig. 2, D and B, respectively), showing that both studied staphylococci planktonic cells are more susceptible to the Chl-API. It can be explained by the fact that during RF-API, I reaction type ROS (e.g. $O_2^{\bullet-}$) prevails, while Chl-APIs are more characterized by $^1O_2$ production [29]. Such conclusions can be supported by the results demonstrated in the previous graphs (Fig. 1, A and B). In the latter it is shown that RF irradiation produced a large amount of $O_2^{\bullet-}$ when irradiated by the blue 440 nm light, while in the case of Chl, near UV 402 nm light did not reach the same level even with a 6-fold dose increase. Thus, it can be assumed that when the bacteria were exposed to low doses of Chl-API, the main damage was initially caused by $^1O_2$ generated outside the cells. The higher levels of $O_2^{\bullet-}$ generated inside the cells when they were exposed to the same dose of RF-API did not have this effect, as these ROS were handled by intracellular enzymes fighting oxidative stress (such as superoxide dismutases). However, these claims require further studies of ROS in bacterial cell suspensions and an additional assay for the detection of $^1O_2$ (e.g. UV–Vis spectroscopy and anthracene or benzofuran).

Samples from corresponding dark controls were gathered and assessed by CFU determination as well. The dark controls, whether with or without investigated PSs, remained relatively stable and exhibited minor fluctuations within acceptable limits during their incubation period parallel to the illumination experiments (Fig. 2, E).

3.2.2. Inactivation of monocultural S. saprophyticus AG1 biofilm

During API studies of *S. saprophyticus* AG1 sessile form, the irradiation doses were varied from 0 to 200 J/cm^2 for both, RF- and Chl-mediated APIs, depending on the biofilm response. Doses of irradiation resulting in a bactericidal effect (reduction of ≥3 $\log_{10}$) against *S. saprophyticus* AG1 monocultural biofilm was determined to be ~140 J/cm^2 (440 nm) and ~75 J/cm^2 (402 nm) when applying RF-

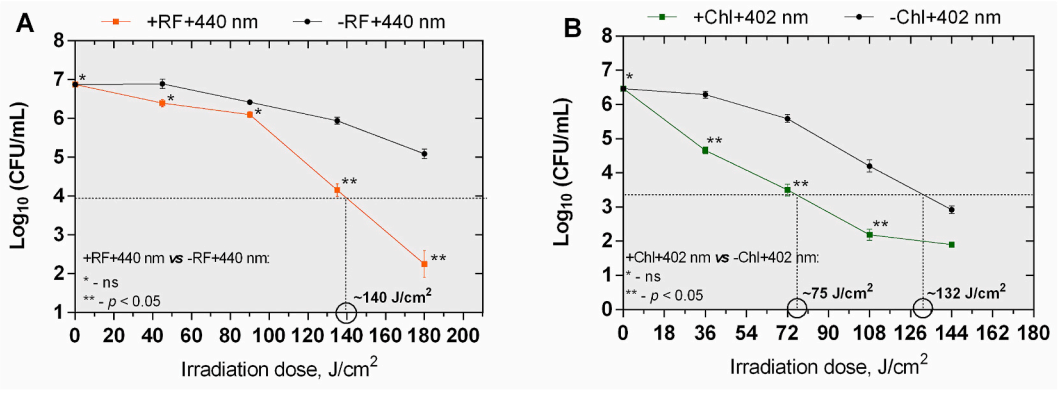

C

Biofilm or sessile form												
	+RF-440 nm* $\log_{10}$ (CFU/mL)						-RF-440 nm** $\log_{10}$ (CFU/mL)					
Incubation time, min / Strain	30	60	90	120	150	180	30	60	90	120	150	180
S. saprophyticus AG1	6.6±0.7	6.5±0.8	6.5±0.7	6.5±0.6	6.4±0.8	6.4±0.9	6.4±1.0	6.4±1.1	6.4±0.2	6.5±0.4	6.3±0.4	6.3±0.4
	+Chl-402 nm* $\log_{10}$ (CFU/mL)						-Chl-402 nm** $\log_{10}$ (CFU/mL)					
Incubation time, min / Strain	30	60	90	120	150	180	30	60	90	120	150	180
S. saprophyticus AG1	6.4±1.0	6.4±0.7	6.5±0.7	6.4±0.8	6.4±0.7	n	6.5±0.1	6.4±0.1	6.5±0.1	6.6±0.1	6.3±0.9	n

Fig. 3. RF-API (**A**) and Chl-API (**B**) of *S. saprophyticus* AG1 biofilm. A horizontal dashed line in the graphs denotes minimal 3 $\log_{10}$ reduction (indicating bactericidal effect). Black circles on the x axis indicate the minimal illumination doses required for the minimal 3 $\log_{10}$ bactericidal effect of the tested bacterial biofilms. ns – non-significant. (**C**) CFU counts of dark controls (reported in $\log_{10}$ scale) of the studied *S. saprophyticus* AG1 biofilms. * - dark control with RF or Chl, respectively; ** - dark control without RF or Chl, respectively; n – was not evaluated; +RF+440 nm *vs* + RF-440 nm and –RF-440 nm or + Chl+402 nm *vs* + Chl-402 nm and –Chl-402 nm p value < 0.05.

and Chl-API, respectively (Fig. 3, A and B).

Chl-API study had also revealed that irradiation at 402 nm had a bactericidal effect on *S. saprophyticus* AG1 biofilm at ~132 J/cm^2 even without Chl. Therefore, the use of PSs, in this case, can be considered redundant to achieve desired antimicrobial effect (Fig. 3, B), however, the effect is observed only when significantly higher doses are used compared to planktonic cells inactivation studies where the light only does not have such effect (Fig. 2). These results clearly show that the efficacy of RF- and Chl-API against the bacteria tested depends on their sensitivity to light itself. This can be attributed to the fact that biofilm cells receive a double hit of ROS when exposed to higher doses of irradiation. This effect is particularly evident with 402 nm light, where the efficiency of Chl-API increases equally with increasing light exposure alone (Fig. 3, B). The susceptibility of biofilms and/or bacterial planktonic cells to the light employed alone (without PS) can be elucidated by the presence of the endogenous photoactivable or light-absorbing porphyrins within bacteria. These porphyrins can lead to generation of ROS upon excitation, subsequently causing damage to a variety of essential cellular macromolecules. Additionally, light can trigger the activation of prophages, resulting in bacterial cell lysis, leading to cell death [68]. It can also be inferred that the cause of the determined susceptibility of the biofilms to the light is somehow associated with their special structural feature - extracellular polymeric matrix (EPM) made of a layer of the exopolysaccharides and other macromolecules (proteins, DNA, lipids etc.) [69]. Moreover, the susceptibility of bacterial biofilm or planktonic cells to API may vary and depend on their metabolic states and the growth phase [70].

Corresponding samples from dark controls were collected and subjected to CFU analysis as well. Dark controls, both with and without PSs, remained relatively stable and exhibited minor fluctuations within acceptable limits during their incubation period, running parallel to the illumination (API) experiments. (Fig. 3, C).

Both RF- and Chl-API were confirmed to have bacteria-killing effects on the free-floating cells of *S. epidermidis* ATCC 12228 and *S. saprophyticus* AG1. However, the doses needed to achieve the effect differed significantly. In general, it was determined that Chl-API was more efficient against tested staphylococci. During Chl-API approximately 150 times lower irradiation doses were required to achieve a 3 $\log_{10}$ CFU reduction of planktonic *S. epidermidis* ATCC 12228 cells and around 22 times lower doses for *S. saprophyticus* AG1 cells. In the case of *S. saprophytocus* AG1 biofilms, the dose to achieve inactivation using Chl-API was ~2 times lower compared to that needed using RF-API.

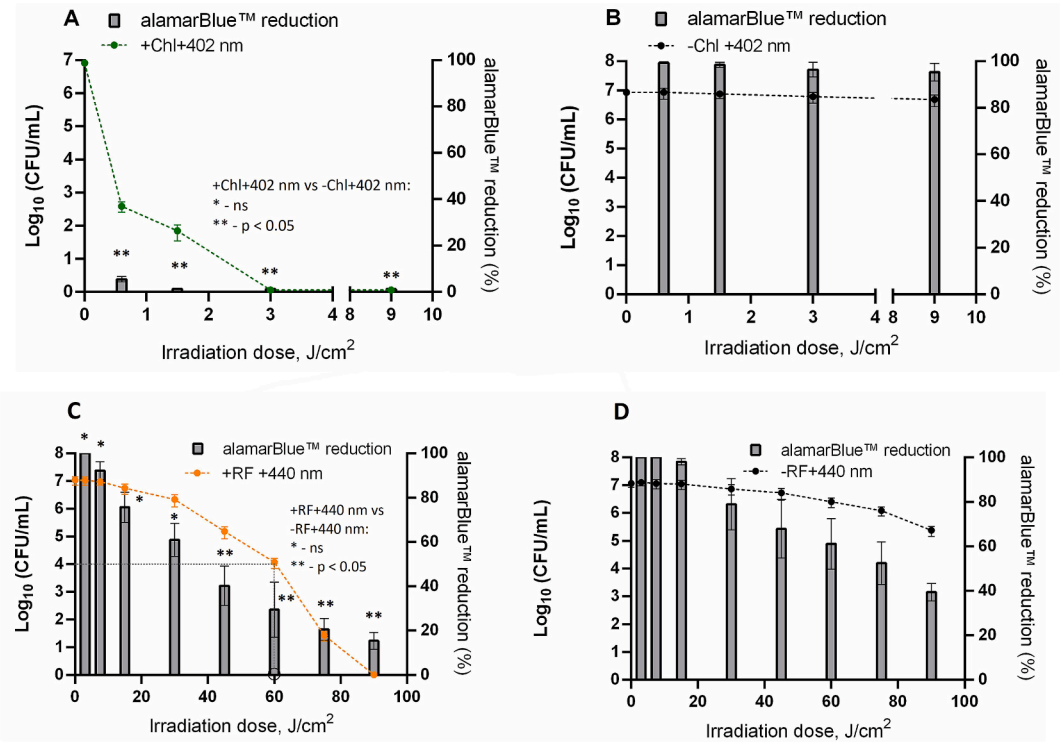

Fig. 4. Ability of the planktonic cells of *S. epidermidis* ATCC 12228 to reduce alamarBlue™ after Chl-API (402 nm at 5 mW/m^2 using appropriate doses) and RF-API (440 nm at 5 mW/m^2 using appropriate doses). Designations: +Chl+402 nm (**A**)/-Chl+402 nm (**B**) - cells irradiated by 402 nm with/without 0.015 mM Chl, respectively; +RF+440 nm (**C**)/–RF+440 nm (**D**) - cells irradiated by 440 nm with/without 0.011 mM RF, respectively. Green (**A**), orange (**C**) and black (**B**, **D**) dashed lines show the changes in the counts of CFU during irradiation with (**A**, **C**) and without (**B**, **D**) Chl/RF, respectively. +Chl +402 nm *vs* dark control groups (+Chl −402 nm; -Chl −402 nm): $p < 0.05$. +RF+440 nm *vs* control groups (+RF-440 nm; -RF-440 nm): $p < 0.05$. (For interpretation of the references to color in this figure legend, the reader is referred to the Web version of this article.)

3.3. alamarBlue™ viability test

Following the RF-mediated and Chl-mediated APIs of the tested staphylococcal free-floating cells and biofilms (the latter was studied in case of *S. saprophyticus* AG1 only) their viability was as well indirectly assessed by analyzing their capacity to reduce the resazurin-based dye alamarBlue™. Indirect measurements of cell viability used so far usually include determination of intracellular ATP, NADH, LDH and proteases. Compared to these metabolic biomarkers or other cytotoxicity assays, alamarBlue™ reagent has the advantage of the capturing reducing environment of living cells only [71]. Inside the cells, the main component of the reagent – resazurin - acts as an indicator to determine whether the samples are growing continuously, where a reducing environment prevails in the cells, or growth is inhibited, where, in such case, an oxidizing environment dominates [72]. Under reducing conditions typical of viable cells, the reagent undergoes modification, rendering it detectable through spectrophotometric or fluorometric measurements due to subsequent color alteration and/or heightened fluorescence. Conversely, non-viable cells do not induce a change in the color of alamarBlue™ [[24,71]].

3.3.1. Differences in the reducing capacity of S. epidermidis ATCC 12228 planktonic cells after Chl- and RF-API

The obtained very low percentage reduction of alamarBlue™ by *S. epidermidis* ATCC 12228 planktonic cells (Fig. 4, A) corresponded to the results obtained by CFU count experiments (Section 3.2.1) and confirmed the results of previous experiments that Chl-API provides a more efficient photodestructive effect on cells. After an irradiation dose of ~0.6 J/cm^2, which corresponded to more than 4 $\log_{10}$ inactivation, the percentage reduction of alamarBlue™ reached only 5.51%. As the irradiation dose increased, cell viability was minimal, with an estimated reduction of less than 1%, which represents greater than 99% inhibition of cell growth (Fig. 4, A and B).

S. epidermidis ATCC 12228 planktonic cells which were exposed only to 402 nm wavelength without using PS Chl, showed greater than 95% alamarBlue™ reduction ability, indicating relatively stable maintenance of viability throughout the experiment (Fig. 4, B). Dark controls were also studied and the reduction ability of these cells after appropriate times of sampling during dark incubation did not change. The data is not shown.

The CFU count and alamarBlue™ reduction ability by the planktonic *S. epidermidis* ATCC 12228 cells which survived after the

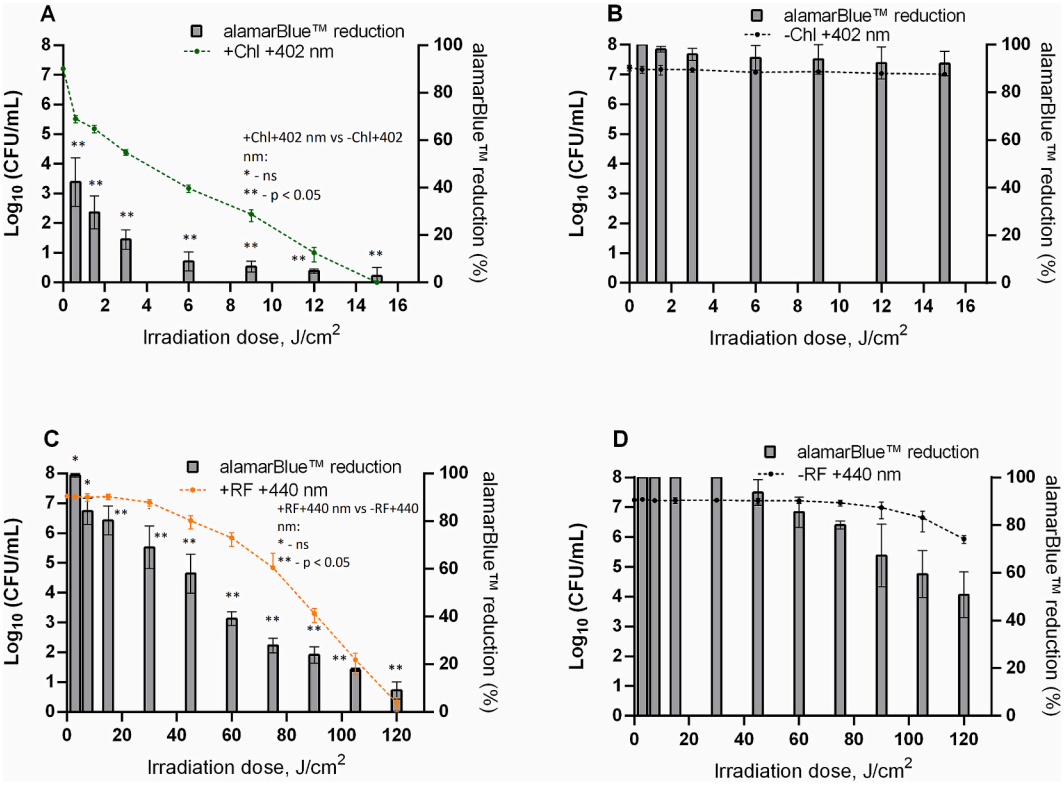

Fig. 5. Ability of the planktonic cells of the *S. saprophyticus* AG1 to reduce alamarBlue™ after Chl- (402 nm at 5 mW/m^2 using appropriate doses) and RF-API (440 nm at 5 mW/m^2 using appropriate doses). Designations: +Chl +402 nm (**A**)/-Chl +402 nm (**B**)/+RF +440 nm (**C**)/–RF +440 nm (**D**) - cells irradiated by 402 nm/440 nm with/without 0.015 mM Chl/0.011 mM RF, respectively. Green (**A**), orange (**C**) and black (**B**, **D**) dashed lines show the changes in the counts of CFU during irradiation with and without Chl (**A**, **B**) or RF (**C**, **D**), respectively. +RF +440 nm/+Chl +402 nm *vs* dark control groups (+Chl – 402 nm/+RF-440 nm; -Chl –402 nm/-RF-440 nm): $p < 0.05$. (For interpretation of the references to color in this figure legend, the reader is referred to the Web version of this article.)

exposure to RF-API have also shown correlation (Fig., 4, C). At an irradiation dose of 60 J/cm^2, corresponding to 3 log$_{10}$ inactivation, alamarBlue™ reduction by remaining metabolically active cells was only 29.46%. From 60 J/cm^2 to 90 J/cm^2, a further decrease in cell viability was recorded. At 90 J/cm^2 irradiation dose CFU were not detected, meanwhile alamarBlue™ reduction activity by the cells was 16.37% indicating that metabolically active cells remained.

Decreasing metabolic activity of *S. epidermidis* ATCC 12228 planktonic cells was also detected when the cells were exposed to increasing irradiation dose by 440 nm wavelength light only (without RF, at 20 J/cm^2) (Fig. 4, D). A trending decrease was recorded from 15 J/cm^2 and up to the 90 J/cm^2 dose, at which alamarBlue™ percentage reduction amounted to 41.36 %.

3.3.2. *Differences in the reducing capacity of S. saprophyticus AG1 planktonic cells and biofilm after Chl- and RF-API*

In the case of the study of *S. saprophyticus* AG1 planktonic cells reducing metabolic activity as a viability indicator after the Chl- and RF-API, it was shown that during Chl-API, with the increase of the irradiation dose, cells significantly lose their ability to reduce alamarBlue™ (Fig. 5, A). The result as well strongly correlates with CFU count studied as the primary selection standard viability test used to determine the effect of the API, including Chl-API (in this case) on *S. saprophyticus* AG1 floating cells. Like the determined reduction capacity of *S. epidermidis* ATCC 12228 the higher efficiency of Chl-API was confirmed. At the start of the measurements of the reducing activity (at irradiation dose of 0.6 J/cm^2) reducing ability of the cells was ~42%, at 3 log$_{10}$ causing irradiation dose ability to reduce the dye fell to ≥20 %, further irradiation caused further decrease in ability to reduce alamarBlue™ up to less than 10% residual reduction activity (Fig. 5, A).

During RF-API, with the increase of the irradiation dose, the ability of the *S. saprophyticus* AG1 planktonic cells to reduce alamarBlue™ decreased (as in the case of *S. epidermidis* ATCC 12228 planktonic cells study (Fig. 5, C). Viability testing by the evaluation of reducing activity correlated with the CFU count results of the cells that survived after the treatment. It was determined that the irradiation dose of 81 J/cm^2 which caused 3 log$_{10}$ CFU count reduction indicating bactericidal effect, have also caused a sharp drop in metabolic process which at the mentioned dose reached only ~20 % reduction activity of alamarBlue™. Further irradiation dose increase caused further drop of reducing activity down to only 9% at 120 J/cm^2 (Fig. 5, C).

Percentage alamarBlue™ reduction activity of *S. saprophyticus* AG1 planktonic cells which were treated only by 402 or 440 nm light

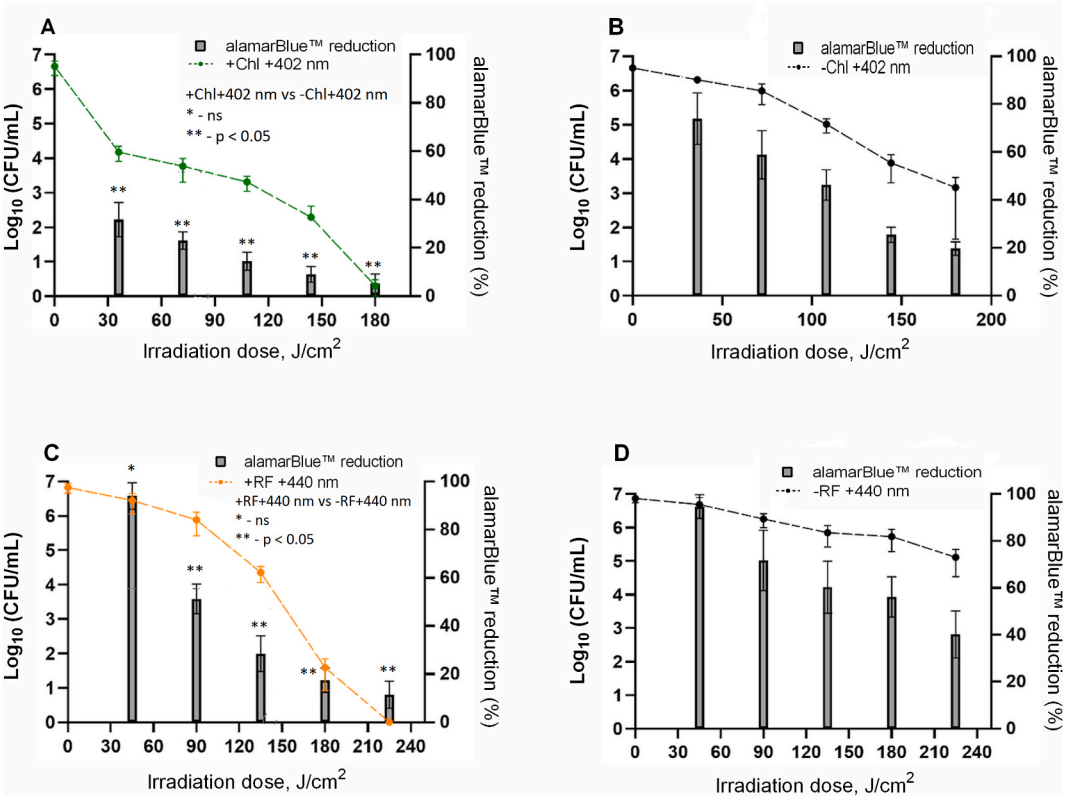

Fig. 6. Ability of *S. saprophyticus* AG1 biofilms to reduce alamarBlue™ after Chl- (402 nm at 5 mW/m^2 using appropriate doses) and RF-API (440 nm at 5 mW/m^2 using appropriate doses). Designations: +Chl +402 nm (A)/-Chl +402 nm (**B**)/+RF +440 nm (**C**)/–RF +440 nm (**D**) - biofilms irradiated by 402 nm/440 nm with/without 0.015 mM Chl/0.011 mM RF, respectively. Green (**A**), orange (**C**) and black (**B**, **D**) dashed lines show the changes in the counts of CFU during irradiation with and without Chl (**A**, **B**) or RF (**C**, **D**), respectively. +RF +440 nm/+Chl +402 nm *vs* control groups (+Chl – 402 nm/+RF-440 nm; -Chl –402 nm/-RF-440 nm): $p < 0.05$. (For interpretation of the references to color in this figure legend, the reader is referred to the Web version of this article.)

without Chl or RF, respectively, remained more than ~80–90% at almost all tested irradiation doses (Fig. 5, B–D), indicating that the light alone does not alter metabolic activity of the cells therefore its viability. Results also correlate with those obtained by counting residual CFU number of the cells.

Assessing the viability of photoinactivated *S. saprophyticus* AG1 biofilm through metabolic reduction activity testing revealed that both Chl-API (with an irradiation dose of approximately 75 J/cm^2) and RF-API (with a dose of around 140 J/cm^2), causing a 3 $\log_{10}$ CFU count reduction, resulted in cellular changes leading to the retention of only about 30% residual alamarBlue™ reduction activity (Fig. 6, A–C). These findings corroborate previously obtained results that *S. saprophyticus* AG1 biofilm after the Chl- and RF-API undergoes significant CFU count or viability loss. Increasing Chl- and RF-API irradiation dose up to 180 J/cm^2 and 225 J/cm^2 only 5.26% reduction activity retained (Fig. 6, A–C).

The biofilm of *S. saprophyticus* AG1, which was exposed solely to 402 nm and 440 nm wavelengths without the use of Chl and RF, respectively, exhibited a gradual decrease in alamarBlue™ reduction ability as the irradiation doses increased (Fig. 6, C and D). This corresponded to a decrease in CFU count under the same conditions.

Study of the dark controls after incubation of planktonic cells and biofilm for appropriate times of incubation with and without PSs (Chl and RF) did not reveal significant alamarBlue™ reduction activity loss and remained at about 90% in all tested samples (data not shown).

After cell inactivation, at some dose points where CFU count was below detection limit (Figs. 2 and 3), metabolic activity of the cells or - alamarBlue™ reduction – was determined (Figs. 4–6). Such results demonstrate the sensitivity of the method, which enables to detect as little as 20 cells per well of a microplate using alamarBlue™ reagent. Also, according to the literature, under specific environmental conditions (usually severe stressors such as starvation, oxidative stress, extreme temperature, irradiation), *Staphylococcus* can switch to viable but non-culturable (VBNC) state. After enabling such an adaptive survival strategy, bacteria in the VBNC state can maintain genetic information, metabolic activity, but cannot divide and form colonies [[73,74]]. Therefore, in any studies where there is a possibility for the cells to switch to the VBNC state, it is suggested to add viability evaluation experiments that would not depend on CFU [75] and therefore, would allow correct interpretation of the results.

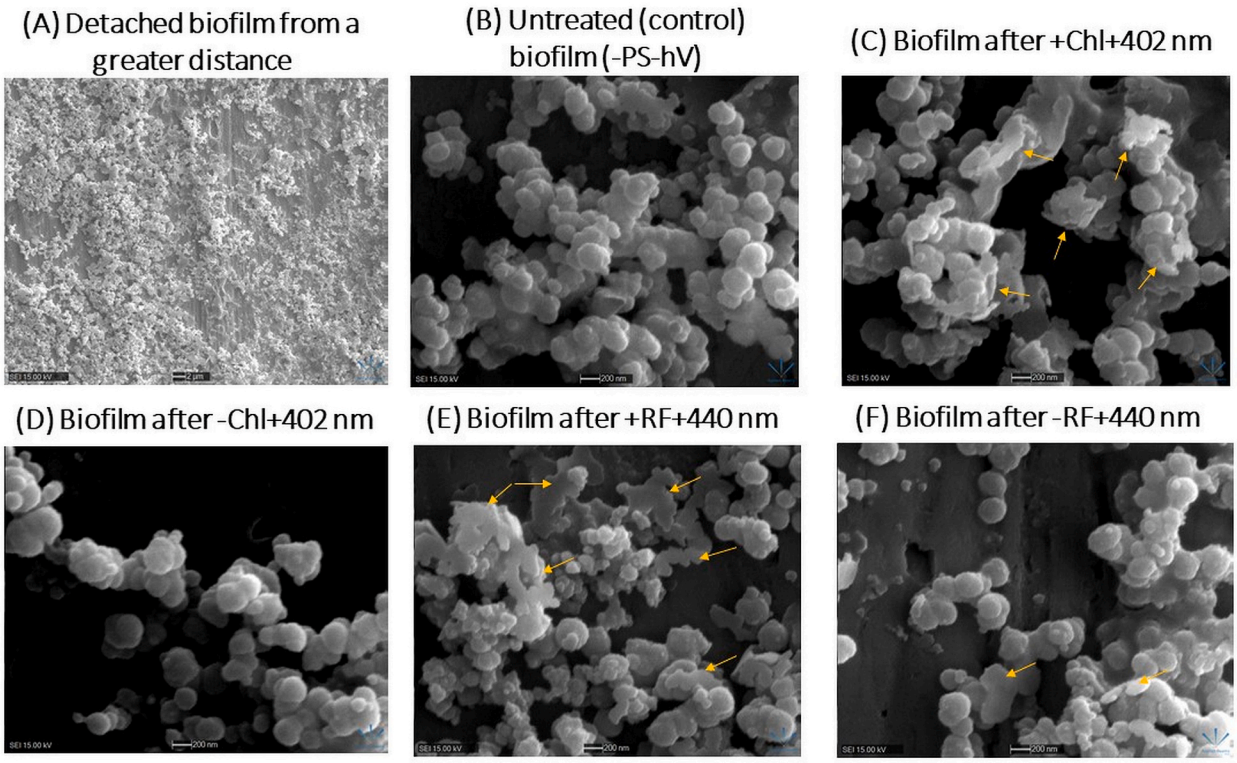

Fig. 7. SEM images of *S. saprophyticus* AG1 biofilm: (**A**) **mechanically detached biofilms from a greater distance;** (**B**) **untreated (control) biofilm (-PS-*hV*) -** no PSs (RF nor Chl) in dark conditions) – incubated for an amount of minutes corresponding to 140 J/cm^2; (**C**) **biofilm after + Chl+402 nm** (treated with 0.015 mM Chl and irradiated by 402 nm up to 75 J/cm^2 – Chl-API dose at which bactericidal effect was determined); (**D**) **biofilm after -Chl+402 nm** (not treated with 0.015 mM Chl prior to irradiation, cells were covered with 0.1 M phosphate buffer (pH 7.4) instead and irradiated by 402 nm up to 75 J/cm^2); (**E**) **biofilm after + RF+440 nm** (treated with 0.011 mM RF and irradiated by 440 nm up to 140 J/cm^2 - RF-API dose at which bactericidal effect was determined); (**F**) **biofilm after -RF+440 nm** (not treated with 0.011 mM RF prior to irradiation, cells were covered with 0.1 M phosphate buffer (pH 7.4) and irradiated by 440 nm up to 140 J/cm^2). Yellow arrows indicate lysed and sloughed, dead staphylococcal biofilm-forming cells. (For interpretation of the references to color in this figure legend, the reader is referred to the Web version of this article.)

It should be also noted that compared to CFU count method, alamarBlue™ dye is added directly to the working buffer solution with photoinactivated cells, without giving them the opportunity to divide and grow on the nutrient medium with the necessary growth factors, excluding possible cell repair mechanisms. In the nutrient media conditions can be favorable for excision repair (dark repair), to occur and many different types of DNA damage can be repaired [76] leading to colony forming even after (sublethal) photoinactivation. Therefore, results obtained after the alamarBlue™ reduction activity measurements can provide a more realistic picture of bacterial cell survival in conditions, where nutrients are absent.

Previous publications investigating the susceptibility of bacterial biofilms, e.g. *S. aureus* [77] or *S. epidermidis* [78] to different antimicrobial methods with alamarBlue™ also confirm the reliability and advantages of the latter, compared to the method of counting CFU. This method, which characterizes metabolic activity, is appreciated for its cost-effectiveness, faster results, and the possibility of continuous monitoring of kinetic in vitro studies of biofilms. All this can facilitate the search for and application of specific antimicrobial agents and methods.

In conclusion, the presented results with alamarBlue™ reduction confirmed the effectiveness of API for the tested *Staphylococcus* strains.

3.4. SEM of photoinactivated biofilms

SEM uncovered that Chl- and RF-mediated API treated biofilms that received an irradiation doses causing 3 $\log_{10}$ CFU count reduction (75 and 140 J/cm^2 using Chl- and RF-API, respectively) and a strong decrease in reductive metabolic activity (described in Section 3.1.1) have also had morphological changes induced by the APIs compared to untreated biofilm (Fig. 7).

Following both Chl-API and RF-API treatment, mechanically detached biofilm-forming cells exhibited disrupted, flattened, visibly damaged cell walls, with some showing signs of lysis (Fig. 7, C–E). SEM analysis also revealed some morphological changes after irradiation with 440 nm without the use of RF (Fig. 7, F). Post-irradiation CFU count has demonstrated that 440 nm light in absence of RF can also exert a diminishing effect on viability: at 140 J/cm^2 a drop of more than 1 $\log_{10}$ in CFU count was determined (Fig. 3, A). This effect can be attributed to the mentioned fact that at high irradiation doses at 440 nm as were used during RF-API, intrinsic ROS species that are also damaging to the cells can be formed. While irradiation with 402 nm light in the absence of Chl also led to a reduction in CFU count (refer to Fig. 3, B), no morphological changes were observed. Additionally, the cells in the dark controls did not exhibit any noticeable damage to the cell walls.

4. Conclusions

Most of the staphylococcal (staph) infections are caused by MRSA and other strains of *S. areus*, however, CNS prevalence and association with HAI is also worrying. In this work we have shown that visible light combined with safe and natural PSs such as Chl and RF (Chl- and RF-mediated API) can inactivate (reaching bactericidal effect) such CNS bacteria as *S. epidermidis* (planktonic cells) and *S. saprophyticus* (planktonic cells and biofilm) with Chl-mediated API being the most efficient in all cases. The residual viability after Chl- and RF-API was determined using classical CFU count method and metabolic function analysis method (alamarBlue™ reduction evaluation method). The results of the reduction capacity of alamarBlue™ obtained during experiments correlated with the CFU count method and confirmed that the determination of viability, which proves the metabolic activity, can be a sensitive substitution for the methods relying on the CFU counts for the evaluation of the activity of antimicrobials and/or even an informative supplement allowing to determine transition of the bacteria to VBNC state. However, to definitively confirm the transition of *Staphylococcus* sp. to VBNC (which is generally a less common phenomenon among Gram-positive bacteria compared to Gram-negative) [79] after the API, such methods as direct microscopic examination (using, e.g., Live/Dead BacLight staining technique), RNA-based methods, such as RT-PCR targeting housekeeping genes and other could be additionally used [80].

The efficacy of API against bacteria hinges on the capacity of the PS and light to generate sufficient ROS, surpassing bacterial defense mechanisms and trigger oxidative stress severe enough to eradicate bacteria. $O_2^{-\bullet}$ is one of the ROS responsible for inducing oxidative stress in bacteria after API. Detecting $O_2^{-\bullet}$ in solution typically requires specialized methods and reagents due to its reactivity. In this study it was determined whether aqueous solutions of used PSs (RF and Chl), when exposed to illumination with optimal exciting light, generate $O_2^{-\bullet}$. After analyzing the reduction of NBT, it was found that after irradiation of both studied PSs, $O_2^{-\bullet}$of type I ROS reactions are formed. The absorbance value of reduced NBT at 560 nm increased with increasing irradiation dose. This means that more $O_2^{-\bullet}$ are formed in the solution. However, their quantity depends on the irradiation dose used and the type of PS that initiates ROS formation reactions upon exposure.

Performed experiments have also shown that when RF was exposed to irradiation with a blue light of 440 nm wavelength, more $O_2^{-\bullet}$ were generated than when Chl was irradiated with near-UV wavelength of 402 nm. Although it increased after applying a 6-fold higher irradiation dose, the amount of $O_2^{-\bullet}$ during irradiation with Chl does not reach the same level as when irradiating with RF. This discussion suggests that the prominent initial antibacterial effect of Chl-API at lower doses might be due to the predomination of $^1O_2$ or other radicals than $O_2^{-\bullet}$. Furthermore, after applying higher doses of light, more $O_2^{-\bullet}$ are observed when Chl is already photodegraded.

Although free radicals such as $O_2^{-\bullet}$ contribute to photodestruction, $^1O_2$ is considered to be the main ROS contributing to cell death in API. Higher doses of irradiation without PS against bacteria can induce a bactericidal effect, but its effectiveness is highly dependent on various intracellular mechanisms of resistance to oxidative stress, such as superoxide dismutases, which are able to combat $O_2^{-\bullet}$. Chl is mentioned as an example of a PS that is particularly effective at generating $^1O_2$ upon excitation [29]. Combining a PS like Chl with irradiation allows for effective bacterial inactivation at lower doses of light. This is beneficial as it minimizes potential damage to surrounding healthy tissues in therapeutic contexts.

Therefore, RF- and Chl-based API can be considered as a very potent and safe antibacterial technology that could prevent CNS-caused nosocomial infections and could be used to protect food systems from spreading foodborne intoxications that are caused not only by *S. aureus* but also *S. saprophyticus* strains.

Funding

Part of the research received funding from the European Space Agency (ESA) (LT5_1 ESA Contract No. 40000129495/19/NL/SSC).

Data availability statement

Data will be made available on request.

CRediT authorship contribution statement

Alisa Gricajeva: Visualization, Validation, Supervision, Software, Resources, Conceptualization, Data curation, Formal analysis, Investigation, Methodology, Writing – original draft, Writing – review & editing. **Irina Buchovec:** Writing – review & editing, Writing – original draft, Validation, Methodology, Formal analysis, Data curation, Conceptualization, Resources. **Lilija Kalėdienė:** Writing – review & editing, Methodology, Formal analysis, Conceptualization. **Kazimieras Badokas:** Methodology. **Pranciškus Vitta:** Writing – review & editing, Supervision, Project administration, Funding acquisition, Formal analysis, Conceptualization.

Declaration of competing interest

The authors declare that they have no known competing financial interests or personal relationships that could have appeared to influence the work reported in this paper.

Acknowledgements

Authors would like to acknowledge students Laura Jurkaitytė and Deimantė Purytė and ESA.

References

[1] M. Widerström, Significance of *Staphylococcus epidermidis* in health care-associated infections, from contaminant to clinically relevant pathogen: this is a wake-up call, J. Clin. Microbiol. 54 (2016) 1679–1681, https://doi.org/10.1128/JCM.00743-16.
[2] V. Siciliano, R.A. Passerotto, M. Chiuchiarelli, G.M. Leanza, V. Ojetti, Difficult-to-treat pathogens: a review on the management of multidrug-resistant *Staphylococcus epidermidis*, Life 13 (2023) 1126, https://doi.org/10.3390/life13051126.
[3] R. Chabi, H. Momtaz, Virulence factors and antibiotic resistance properties of the *Staphylococcus epidermidis* strains isolated from hospital infections in Ahvaz, Iran, Trop. Med. Health 47 (2019) 56, https://doi.org/10.1186/s41182-019-0180-7.
[4] N.E. Natsis, P.R. Cohen, Coagulase-negative *Staphylococcus* skin and soft tissue infections, Am. J. Clin. Dermatol. 19 (2018) 671–677, https://doi.org/10.1007/s40257-018-0362-9.
[5] G. Pietrocola, D. Campoccia, C. Motta, L. Montanaro, C.R. Arciola, P. Speziale, Colonization and infection of indwelling medical devices by *Staphylococcus aureus* with an emphasis on orthopedic implants, Int. J. Mol. Sci. 23 (2022) 5958, https://doi.org/10.3390/ijms23115958.
[6] J.R. Hindy, S.F. Haddad, S.S. Kanj, New drugs for methicillin-resistant *Staphylococcus aureus* skin and soft tissue infections, Curr. Opin. Infect. Dis. 35 (2022) 112–119, https://doi.org/10.1097/QCO.0000000000000800.
[7] C. Heilmann, W. Ziebuhr, K. Becker, Are coagulase-negative staphylococci virulent? Clin. Microbiol. Infect. 25 (2019) 1071–1080, https://doi.org/10.1016/j.cmi.2018.11.012.
[8] Y. Zheng, L. He, T.K. Asiamah, M. Otto, Colonization of medical devices by staphylococci, Environ. Microbiol. 20 (2018) 3141–3153, https://doi.org/10.1111/1462-2920.14129.
[9] K. Becker, A. Both, S. Weißelberg, C. Heilmann, H. Rohde, Emergence of coagulase-negative staphylococci, Expert Rev. Anti Infect. Ther. 18 (2020) 349–366, https://doi.org/10.1080/14787210.2020.1730813.
[10] R. Michels, K. Last, S.L. Becker, C. Papan, Update on coagulase-negative staphylococci-what the clinician should know, Microorganisms 9 (2021) 830, https://doi.org/10.3390/microorganisms9040830.
[11] M. Van Kerckhoven, A. Hotterbeekx, E. Lanckacker, P. Moons, C. Lammens, M. Kerstens, M. Ieven, P. Delputte, P.G. Jorens, S. Salhotra-Kumar, H. Goossens, L. Maes, P. Cos, Characterizing the in vitro biofilm phenotype of *Staphylococcus epidermidis* isolates from central venous catheters, J. Microbiol. Methods 127 (2016) 95–101, https://doi.org/10.1016/j.mimet.2016.05.009.
[12] F. Gomes, P. Teixeira, R. Oliveira, Mini-review: *Staphylococcus epidermidis* as the most frequent cause of nosocomial infections: old and new fighting strategies, Biofouling 30 (2014) 131–141, https://doi.org/10.1080/08927014.2013.848858.
[13] S. Ehlers, S.A. Merrill, *Staphylococcus saprophyticus* infection, in: StatPearls [Internet], StatPearls Publishing, Treasure Island (FL), 2023.
[14] O.U. Lawal, M. Barata, M.J. Fraqueza, P. Worning, M.D. Bartels, L. Goncalves, P. Paixão, E. Goncalves, C. Toscano, J. Empel, M. Urbaś, M.A. Domìnguez, H. Westh, H. de Lencastre, M. Miragaia, *Staphylococcus saprophyticus* from clinical and environmental origins have distinct biofilm composition, Front. Microbiol. 12 (2021) 663768, https://doi.org/10.3389/fmicb.2021.663768.
[15] O.U. Lawal, M.J. Fraqueza, P. Worning, O. Bouchami, M.D. Bartels, L. Goncalves, P. Paixão, E. Goncalves, C. Toscano, J. Empel, M. Urbaś, M.A. Domínguez, H. Westh, H. de Lencastre, M. Miragaia, *Staphylococcus saprophyticus* causing infections in humans is associated with high resistance to heavy metals, Antimicrob. Agents Chemother. 65 (2021) e0268520, https://doi.org/10.3201/eid2703.200852.
[16] C. Pérez, T. Zúñiga, C.E. Palavecino, Photodynamic therapy for treatment of *Staphylococcus aureus* infections, Photodiagnosis Photodyn. Ther. 34 (2021) 102285, https://doi.org/10.1016/j.pdpdt.2021.102285.
[17] M. Wainwright, T. Maisch, S. Nonell, K. Plaetzer, A. Almeida, G.P. Tegos, M.R. Hamblin, Photoantimicrobials—are we afraid of the light? Lancet Infect. Dis. 17 (2017) 49–55. https://doi:10.1016/S1473-3099(16)30268-7.
[18] J. Ghorbani, D. Rahban, S. Aghamiri, A. Teymouri, A. Bahador, Photosensitizers in antibacterial photodynamic therapy: an overview, Laser Ther. 27 (2018) 293–302, https://doi.org/10.5978/islsm.27_18-RA-01.

[19] J. Nakonieczna, E. Michta, M. Rybicka, M. Grinholc, A. Gwizdek-Wiśniewska, K.P. Bielawski, Superoxide dismutase is upregulated in *Staphylococcus aureus* following protoporphyrin-mediated photodynamic inactivation and does not directly influence the response to photodynamic treatment, BMC Microbiol. 10 (2010) 323, https://doi.org/10.1186/1471-2180-10-323.

[20] C.M.C. Andrés, J.M. Pérez de la Lastra, C. Andrés Juan, F.J. Plou, E. Pérez-Lebeña, Superoxide anion Chemistry-its role at the Core of the Innate Immunity, Int. J. Mol. Sci. 24 (2023) 1841, https://doi.org/10.3390/ijms24031841.

[21] M.I. Heller, P.L. Croot, Application of a superoxide (O(2)(-)) thermal source (SOTS-1) for the determination and calibration of O(2)(-) fluxes in seawater, Anal. Chim. Acta 667 (2010) 1–13, https://doi.org/10.1016/j.aca.2010.03.054.

[22] R.O. Olojo, R.H. Xia, J.J. Abramson, Spectrophotometric and fluorometric assay of superoxide ion using 4-chloro-7-nitrobenzo-2-oxa-1,3-diazole, Anal. Biochem. 339 (2005) 338–344, https://doi.org/10.1016/j.ab.2005.01.032.

[23] A. Rapacka-Zdonczyk, A. Wozniak, J. Nakonieczna, M. Grinholc, Development of antimicrobial phototreatment tolerance: why the methodology matters, Int. J. Mol. Sci. 22 (2021) 2224, https://doi.org/10.3390/ijms22042224.

[24] A. Gricajeva, I. Buchovec, L. Kalėdienė, K. Badokas, P. Vitta, Riboflavin- and chlorophyllin-based antimicrobial photoinactivation of *Brevundimonas* sp. ESA1 biofilms, Front. Cell. Infect. Microbiol. 12 (2022) 1006723, https://doi.org/10.3389/fcimb.2022.1006723.

[25] Y. Liu, R. Qin, S.A.J. Zaat, E. Breukink, M. Heger, Antibacterial photodynamic therapy: overview of a promising approach to fight antibiotic-resistant bacterial infections, J. Clin. Transl. Res. 1 (2015) 140–167, https://doi.org/10.18053/jctres.201503.002.

[26] T. Maisch, Resistance in antimicrobial photodynamic inactivation of bacteria, Photochem. Photobiol. Sci. 14 (2015) 1518–1526, https://doi.org/10.1039/c5pp00037h.

[27] N. Kashef, M.R. Hamblin, Can microbial cells develop resistance to oxidative stress in antimicrobial photodynamic inactivation? Drug Resist. Updates 31 (2017) 31–42, https://doi.org/10.1016/j.drup.2017.07.003.

[28] I. Buchovec, A. Gricajeva, L. Kalėdienė, P. Vitta, Antimicrobial photoinactivation approach based on natural agents for control of bacteria biofilms in spacecraft, Int. J. Mol. Sci. 21 (2020) 6932, https://doi.org/10.3390/ijms21186932.

[29] I. Buchovec, V. Lukseviciūtė, R. Kokstaite, D. Labeikyte, L. Kaziukonyte, Z. Luksiene, Inactivation of gram (–) bacteria *Salmonella enterica* by chlorophyllin-based photosensitization: mechanism of action and new strategies to enhance the inactivation efficiency, J. Photochem. Photobiol. B Biol. 172 (2017) 1–10, https://doi.org/10.1016/j.jphotobiol.2017.05.008.

[30] M. Krüger, P.R. Richter, S.M. Strauch, A. Nasir, A. Burkovski, C.A. Antunes, T. Meißgeier, E. Schlücker, S. Schwab, M. Lebert, What an *Escherichia coli* mutant can teach us about the antibacterial effect of chlorophyllin, Microorganisms 7 (2019) 59, https://doi.org/10.3390/microorganisms7020059.

[31] Z. Luksiene, I. Buchovec, Impact of chlorophyllin-chitosan coating and visible light on the microbial contamination, shelf life, nutritional and visual quality of strawberries, Innovat. Food Sci. Emerg. Technol. 52 (2019) 463–472, https://doi.org/10.1016/j.ifset.2019.02.003.

[32] I. Buchovec, L. Klimkaitė, E. Sužiedėlienė, S. Bagdonas, Inactivation of opportunistic pathogens *Acinetobacter baumannii* and *Stenotrophomonas maltophilia* by antimicrobial photodynamic therapy, Microorganisms 10 (2022) 506, https://doi.org/10.3390/microorganisms10030506.

[33] S. Astanov, M.Z. Sharipov, A.R. Fayzullaev, E.N. Kurtaliev, N. Nizomov, Spectroscopic study of photo and thermal destruction of riboflavin, J. Mol. Struct. 1071 (2014) 133–138, https://doi.org/10.1016/j.molstruc.2014.04.077.

[34] M.A. Sheraz, S.H. Kazi, S. Ahmed, Z. Anwar, I. Ahmad, Photo, thermal and chemical degradation of riboflavin, Beilstein J. Org. Chem. 10 (2014) (2014) 1999–2012, https://doi.org/10.3762/bjoc.10.208.

[35] F. Halili, A. Arboleda, H. Durkee, M. Taneja, D. Miller, K.A. Alawa, M.C. Aguilar, G. Amescua, H.W. Flynn Jr., J.M. Parel, Rose bengal- and riboflavin-mediated photodynamic therapy to inhibit methicillin-resistant *Staphylococcus aureus* keratitis isolates, Am. J. Ophthalmol. 166 (2016) 194–202, https://doi.org/10.1016/j.ajo.2016.03.014.

[36] K. Makdoumi, M. Hedin, A. Bäckman, Different photodynamic effects of blue light with and without riboflavin on methicillin-resistant *Staphylococcus aureus* (MRSA) and human keratinocytes *in vitro*, Laser Med. Sci. 34 (2019) 1799–1805, https://doi.org/10.1007/s10103-019-02774-9.

[37] P.S. Thakuri, R. Joshi, S. Basnet, S. Pandey, S.D. Taujale, N. Mishra, Antibacterial photodynamic therapy on *Staphylococcus aureus* and *Pseudomonas aeruginosa in-vitro*, Nepal Med. Coll. J. 13 (2011) 281–284.

[38] S. Banerjee, D. Ghosh, K. Vishakha, S. Das, S. Mondal, A. Ganguli, Photodynamic antimicrobial chemotherapy (PACT) using riboflavin inhibits the mono and dual species biofilm produced by antibiotic resistant *Staphylococcus aureus* and *Escherichia col*, Photodiagnosis Photodyn. Ther. 32 (2020) 102002, https://doi.org/10.1016/j.pdpdt.2020.102002.

[39] Y. Yan, L. Tan, H. Li, B. Chen, J. Huang, Y. Zhao, J. Wang, J. Ou, Photodynamic inactivation of planktonic *Staphylococcus aureus* by sodium magnesium chlorophyllin and its effect on the storage quality of lettuce, Photochem. Photobiol. Sci. 20 (2021) 761–771, https://doi.org/10.1007/s43630-021-00057-3.

[40] G. López-Carballo, P. Hernández-Muñoz, R. Gavara, M.J. Ocio, Photoactivated chlorophyllin-based gelatin films and coatings to prevent microbial contamination of food products, Int. J. Food Microbiol. 126 (2008) 65–70, https://doi.org/10.1016/j.ijfoodmicro.2008.05.002.

[41] A.R.L. Caires, V.A. Nascimento, Photoinactivation effect of eosin methylene blue and chlorophyllin sodium-copper against *Staphylococcus aureus* and *Escherichia coli*, Laser Med. Sci. 32 (2017) 1081–1088, https://doi.org/10.1007/s10103-017-2210-1.

[42] P. Phasupan, T.D. Le, L.T. Nguyen, Assessing the photodynamic efficacy of different photosensitizer-light treatments against foodborne bacteria based on the number of absorbed photons, J. Photochem. Photobiol., B 221 (2021) 112249, https://doi.org/10.1016/j.jphotobiol.2021.112249.

[43] M. Hasenleitner, K. Plaetzer, In the right light: photodynamic inactivation of microorganisms using a LED-based illumination device tailored for the antimicrobial application, Antibiotics 9 (2019) 13, https://doi.org/10.3390/antibiotics9010013.

[44] C.S.A. Caires, C.M. Silva, A.R. Lima, L.M. Alves, T.H.N. Lima, A.C.S. Rodrigues, M.R. Chang, S.L. Oliveira, C. Whitby, V.A. Nascimento, A.R.L. Caires, Photodynamic inactivation of methicillin-resistant *Staphylococcus aureus* by a natural food colorant (E-141ii), Molecules 25 (2020) 4464, https://doi.org/10.3390/molecules25194464.

[45] H.H. Buzzá, F. Alves, A.J.B. Tomé, J. Chen, G. Kassab, J. Bu, V.S. Bagnato, G. Zheng, C. Kurachi, Porphyrin nanoemulsion for antimicrobial photodynamic therapy: effective delivery to inactivate biofilm-related infections, Proc. Natl. Acad. Sci. U.S.A. 119 (2022) e2216239119, https://doi.org/10.1073/pnas.2216239119.

[46] M. Sharma, L. Visai, F. Bragheri, I. Cristiani, P.K. Gupta, P. Speziale, Toluidine blue-mediated photodynamic effects on staphylococcal biofilms, Antimicrob. Agents Chemother. 52 (2008) 299–305, https://doi.org/10.1128/AAC.00988-07.

[47] E. Darabpour, N. Kashef, S.M. Amini, S. Kharrazi, G.E. Djavid, Fast and effective photodynamic inactivation of 4-day-old biofilm of methicillin-resistant *Staphylococcus aureus* using methylene blue-conjugated gold nanoparticles, J. Drug Deliv. Sci. Technol. 37 (2017) 134–140, https://doi.org/10.1016/j.jddst.2016.12.007.

[48] M. Qi, M. Chi, X. Sun, X. Xie, M.D. Weir, T.W. Oates, Y. Zhou, L. Wang, Y. Bai, H.H. Xu, Novel nanomaterial-based antibacterial photodynamic therapies to combat oral bacterial biofilms and infectious diseases, Int. J. Nanomed. 14 (2019) 6937–6956, https://doi.org/10.2147/IJN.S212807.

[49] E. Reynoso, D.D. Ferreyra, E.N. Durantini, M.B. Spesia, Photodynamic inactivation to prevent and disrupt *Staphylococcus aureus* biofilm under different media conditions, Photodermatol. Photoimmunol. Photomed. 35 (2019) 322–331, https://doi.org/10.1111/phpp.12477.

[50] N. Masiera, A. Bojarska, I. Gawryszewska, E. Sadowy, W. Hryniewicz, J. Waluk, Antimicrobial photodynamic therapy by means of porphycene photosensitizers, J. Photochem. Photobiol., B 174 (2017) 84–89, https://doi.org/10.1016/j.jphotobiol.2017.07.016.

[51] L. Mamone, D.D. Ferreyra, L. Gándara, G. Di Venosa, P. Vallecorsa, D. Sáenz, G. Calvo, A. Batlle, F. Buzzola, E.N. Durantini, A. Casas, Photodynamic inactivation of planktonic and biofilm growing bacteria mediated by a meso-substituted porphyrin bearing four basic amino groups, J. Photochem. Photobiol., B 161 (2016) 222–229, https://doi.org/10.1016/j.jphotobiol.2016.05.026.

[52] H. Kariminezhad, M. Mousapour, S. Khorram, H. Amani, Photodynamic inactivation of *Staphylococcus epidermidis*: application of PEGylated gold nanoparticles, Arabian J. Sci. Eng. 45 (2020) 71–79, https://doi.org/10.1007/s13369-019-04248-0.

[53] W.C. de Melo, P. Avci, M.N. de Oliveira, A. Gupta, D. Vecchio, M. Sadasivam, R. Chandran, Y.Y. Huang, R. Yin, L.R. Perussi, G.P. Tegos, J.R. Perussi, T. Dai, M. R. Hamblin, Photodynamic inactivation of biofilm: taking a lightly colored approach to stubborn infection, Expert Rev. Anti Infect. Ther. 11 (2013) 669–693, https://doi.org/10.1586/14787210.2013.811861.

[54] J. Hadi, S. Wu, G. Brightwell, Antimicrobial blue light versus pathogenic bacteria: mechanism, application in the food industry, hurdle technologies and potential resistance, Foods 9 (2020) 1895, https://doi.org/10.3390/foods9121895.
[55] W. Yang, Z. Wang, Q. Li, Y. Jia, S. Song, Z. Ma, J. Liu, J. Wang, Photodynamic inactivation using natural bioactive compound prevents and disrupts the biofilm produced by *Staphylococcus saprophyticus*, Molecules 26 (2021) 4713, https://doi.org/10.3390/molecules26164713.
[56] Z. Wang, Y. Jia, W. Li, M. Zhang, Antimicrobial photodynamic inactivation with curcumin against *Staphylococcus saprophyticus*, in vitro and on fresh dough sheet, Lebensm. Wiss. Technol. 147 (2021) 111567, https://doi.org/10.1016/j.lwt.2021.111567.
[57] C.W. Cheng, L.Y. Chen, C.W. Chou, J.Y. Liang, Investigations of riboflavin photolysis via coloured light in the nitro blue tetrazolium assay for superoxide dismutase activity, J. Photochem. Photobiol., B 148 (2015) 262–267, https://doi.org/10.1016/j.jphotobiol.2015.04.028.
[58] J.Y. Liang, J.P. Yuann, Z.J. Hsie, S.T. Huang, C.C. Chen, Blue light induced free radicals from riboflavin in degradation of crystal violet by microbial viability evaluation, J. Photochem. Photobiol., B 174 (2017) (2017) 355–363, https://doi.org/10.1016/j.jphotobiol.2017.08.018.
[59] J.Y. Liang, J.M. Yuann, C.W. Cheng, H.L. Jian, C.C. Lin, L.Y. Chen, Blue light induced free radicals from riboflavin on *E. coli* DNA damage, J. Photochem. Photobiol., B 119 (2013) 60–64, https://doi.org/10.1016/j.jphotobiol.2012.12.007.
[60] Y.Q. Zhang, S.X. Ren, H.L. Li, Y.X. Wang, G. Fu, J. Yang, Z.Q. Qin, Y.G. Miao, W.Y. Wang, R.S. Chen, Y. Shen, Z. Chen, Z.H. Yuan, G.P. Zhao, D. Qu, A. Danchin, Y.M. Wen, Genome-based analysis of virulence genes in a non-biofilm-forming *Staphylococcus epidermidis* strain (ATCC 12228), Mol. Microbiol. 49 (6) (2003) 1577–1593, https://doi.org/10.1046/j.1365-2958.2003.03671.x.
[61] A. Gricajeva, I. Bikutė, L. Kalėdienė, Atypical organic-solvent tolerant bacterial hormone sensitive lipase-like homologue EstAG1 from *Staphylococcus saprophyticus* AG1: synthesis and characterization, Int. J. Biol. Macromol. 130 (2019) 253–265, https://doi.org/10.1016/j.ijbiomac.2019.02.110.
[62] J.H. Merritt, D.E. Kadouri, G.A. O'Toole, Growing and analyzing static biofilms, Curr. Protoc. Microbiol. 1 (2005), https://doi.org/10.1002/9780471729259.mc01b01s00, 1B.1.
[63] M.P. Trotonda, S. Tamber, G. Memmi, A.L. Cheung, MgrA represses biofilm formation in *Staphylococcus aureus*, Infect. Immun. 76 (2008) 5645–5654, https://doi.org/10.1128/iai.00735-08.
[64] M. Insińska-Rak, M. Sikorski, Riboflavin interactions with oxygen—a survey from the photochemical perspective, Chem. Eur J. 20 (2014) 15280–15291, https://doi.org/10.1002/chem.201403895.
[65] B. Žudytė, M. Velička, V. Šablinskas, Ž. Lukšienė, Understanding *Escherichia coli* damages after chlorophyllin-based photosensitization, J. Biophot. 13 (2020) e202000144, https://doi.org/10.1002/jbio.202000144.
[66] C. Thornsberry, NCCLS standards for antimicrobial susceptibility tests, Lab. Med. 14 (1983) 549–553, https://doi.org/10.1093/labmed/14.9.549.
[67] Clinical and Laboratory Standards Institute (CLSI), Methods for determining bactericidal activity of antimicrobial agents; approved guideline, CLSI document M26-A 19 (18) (1999) 1–29.
[68] R. Ferrer-Espada, X. Liu, X.S. Goh, T. Dai, Antimicrobial blue light inactivation of polymicrobial biofilms, Front. Microbiol. 10 (2019) 721, https://doi.org/10.3389/fmicb.2019.00721.
[69] H.C. Flemming, J. Wingender, The biofilm matrix, Nat. Rev. Microbiol. 8 (2010) 623–633, https://doi.org/10.1038/nrmicro2415.
[70] J.A. Blee, I.S. Roberts, T.A. Waigh, Membrane potentials, oxidative stress and the dispersal response of bacterial biofilms to 405 nm light, Phys. Biol. 17 (3) (2020) 036001, https://doi.org/10.1088/1478-3975/ab759a.
[71] S.N. Rampersad, Multiple applications of alamar blue as an indicator of metabolic function and cellular health in cell viability bioassays, Sensors 12 (2012) 12347–12360, https://doi.org/10.3390/s120912347.
[72] F. Bonnier, M.E. Keating, T.P. Wróbel, K. Majzner, M. Baranska, A. Garcia-Munoz, A. Blanco, H.J. Byrne, Cell viability assessment using the alamar blue assay: a comparison of 2D and 3D cell culture models, Toxicol. Vitro 29 (2015) 124–131, https://doi.org/10.1016/j.tiv.2014.09.014.
[73] Y. Li, T.Y. Huang, Y. Mao, Y. Chen, F. Shi, R. Peng, J. Chen, L. Yuan, C. Bai, L. Chen, K. Wang, J. Liu, Study on the viable but non-culturable (VBNC) state formation of *Staphylococcus aureus* and its control in food system, Front. Microbiol. 11 (2020) 599739, https://doi.org/10.3389/fmicb.2020.599739.
[74] X. Zhao, J. Zhong, C. Wei, C.W. Lin, T. Ding, Current perspectives on viable but non-culturable state in foodborne pathogens, Front. Microbiol. 8 (2017) 580, https://doi.org/10.3389/fmicb.2017.00580.
[75] K. Hoenes, R. Bauer, B. Spellerberg, M. Hessling, Microbial photoinactivation by visible light results in limited loss of membrane integrity, Antibiotics 10 (2021) 341, https://doi.org/10.3390/antibiotics10030341.
[76] K. Fitzhenry, E. Clifford, N. Rowan, A. Val del Rio, Bacterial inactivation, photoreactivation and dark repair post flow-through pulsed UV disinfection, J. Water Process Eng. 41 (2021) 102070, https://doi.org/10.1016/j.jwpe.2021.102070.
[77] R.K. Pettit, C.A. Weber, G.R. Pettit, Application of a high throughput Alamar blue biofilm susceptibility assay to *Staphylococcus aureus* biofilms, Ann. Clin. Microbiol. Antimicrob. 8 (2009) 28, https://doi.org/10.1186/1476-0711-8-28.
[78] R.K. Pettit, C.A. Weber, M.J. Kean, H. Hoffmann, G.R. Pettit, R. Tan, K.S. Franks, M.L. Horton, Microplate Alamar blue assay for *Staphylococcus epidermidis* biofilm susceptibility testing, Antimicrob. Agents Chemother. 49 (2005) 2612–2617, https://doi.org/10.1128/AAC.49.7.2612-2617.2005.
[79] M. Fakruddin, K.S. Mannan, S. Andrews, Viable but nonculturable bacteria: food safety and public health perspective, ISRN Microbiol V2013 (2013) 703813, https://doi.org/10.1155/2013/703813.
[80] J. Liu, L. Yang, B.V. Kjellerup, Z. Xu, Viable but nonculturable (VBNC) state, an underestimated and controversial microbial survival strategy, Trends Microbiol. 31 (10) (2023) P1013–P1023, https://doi.org/10.1016/j.tim.2023.04.009.